doi: 10.18323/2782-4039-2025-2-72-6

Interrelation between the microstructure and impact toughness of the interface of welded joints of 32HGMA and 40HN2MA steels produced by rotary friction welding

Elena Yu. Priymak*[1,2,4], PhD (Engineering), Associate Professor,
Head of the Laboratory of Metal Science and Heat Treatment,
Director of Research and Educational Center of New Materials and Advanced Technologies
Artem S. Atamashkin[2,5], PhD (Engineering), senior researcher
of Research and Educational Center of New Materials and Advanced Technologies
Irina L. Yakovleva[3,6], Doctor of Sciences (Engineering), chief researcher
of the Laboratory of Physical Metallurgy
Andrey P. Fot[1,7], Doctor of Sciences (Engineering), Professor,
Chief Scientific Secretary – Head of Department of Dissertation Councils
[1]*ZBO Drill Industries, Inc., Orenburg (Russia)*
[2]*Orenburg State University, Orenburg (Russia)*
[3]*M.N. Mikheev Institute of Metal Physics of the Ural Branch of RAS, Yekaterinburg (Russia)*

***E-mail:** e.prijmak@zbo.ru

[4]ORCID: https://orcid.org/0000-0002-4571-2410
[5]ORCID: https://orcid.org/0000-0003-3727-8738
[6]ORCID: https://orcid.org/0000-0001-8918-3066
[7]ORCID: https://orcid.org/0000-0002-2971-7908

Received 27.02.2025 *Revised 21.03.2025* *Accepted 10.04.2025*

Abstract: This paper covers the assessment of the influence of the morphological features of the microstructure of medium-carbon alloyed steels, formed at different forces in the process of rotary friction welding (RFW), on the impact toughness of their interface. The paper presents the results of an experimental study of a joint produced by welding tubular billets of 32HGMA and 40HN2MA steels with an outer diameter of 73 mm and a wall thickness of 9 mm with a change in force at the stage of friction (heating) of the billets. The studies of the microstructure, microhardness and impact toughness on samples with a V-notch of welded joints were carried out in the initial state after welding and after tempering at a temperature of 550 °C. Macro- and microfractographic analysis of the destroyed samples was carried out. The study shows that the friction force affects the kinetics of phase transformations, phase composition and microstructure homogeneity in the steel junction zone. With a decrease in this parameter of rotational friction welding, the microstructure heterogeneity associated with the occurrence of upper bainite areas with uneven precipitation of large carbide particles increases, which has a negative effect on the viscosity of the steel interface both in the initial state and after tempering; the fracture mechanism is quasi-cleavage. At higher values of the friction force, the density of high-angle boundaries and the dispersion of the bainite microstructure increase, which ensures higher viscosity and energy capacity of destruction with the formation of a pitted microrelief. The obtained results open up space for regulating the visco-plastic properties of welded joints even at the welding stage without subsequent recrystallisation of the weld zone.

Keywords: rotary friction welding; medium-carbon alloyed steels; welded joint interface; martensite; bainite; impact toughness.

Acknowledgements: The study was supported by the grant of the Russian Science Foundation No. 23-79-01311, https://rscf.ru/project/23-79-01311.

Electron microscope investigations using the electron backscatter diffraction method were carried out at the Center for Collective Use “Testing Center for Nanotechnologies of Advanced Materials” of the Institute of Metal Physics of the Ural Branch of the Russian Academy of Sciences.

Studies using the Tescan Mira 3 scanning electron microscope were carried out at the Center for Collective Use of the Center for Identification and Support of Gifted Children “Gagarin” (Orenburg Region).

For citation: Priymak E.Yu., Atamashkin A.S., Yakovleva I.L., Fot A.P. Interrelation between the microstructure and impact toughness of the interface of welded joints of 32HGMA and 40HN2MA steels produced by rotary friction welding. *Frontier Materials & Technologies*, 2025, no. 2, pp. 73–85. DOI: 10.18323/2782-4039-2025-2-72-6.

INTRODUCTION

The efficiency of geological exploration and major repairs of oil wells depends on the reliability of the drill string. Development of deep wells requires a reduction in the weight of drill pipes, which can be achieved by using stronger steels with a decrease in wall thickness. 26H1MF, 32HMA, 32HGMA and other low- and medium-carbon steels alloyed with Cr, Mo and Mn to achieve an optimal combination of strength and ductility are widely used as the material for the drill pipe body [1–3]. As the material for locking parts, steels with a high carbon content are commonly used to further increase the strength, rigidity and wear resistance of the threaded connections used to assemble the drill string. They include 40HN, 40HN2MA and other steels [4; 5].

The connection of the lock part to the pipe body is usually carried out by means of rotary friction welding (RFW). This method allows joining difficult-to-weld materials, which include medium-carbon alloyed steels used for drill pipes. RFW has a number of technological advantages; the key ones are high productivity, the degree of automation and stability of the quality of welded joints [6–8].

Currently, there are two RFW methods: continuous drive friction welding (conventional), and inertia friction welding. The main difference between these options is the method of supplying the energy required for welding.

During continuous drive RFW, one of the billets is rotated by an electric motor shaft. The billet is rotated at a constant speed and is pressed against a stationary billet with a certain force, resulting in heating of the contact surfaces. When a certain degree of deformation (upset) is reached or after a specified time, the rotating billet quickly stops, and an increased axial forging force is applied to the billets. Cooling after welding is carried out in still air. The resulting burr is removed by mechanical treatment both from the outside and from the inside.

It is known that during rotary friction welding of steels, the billets are heated to the temperature of austenite formation, which undergoes a $\gamma \rightarrow \alpha$ transformation upon completion of the process [9; 10]. The degree of transformation is determined by both the chemical composition of steels and the technological parameters of welding. It is obvious that the applied force during friction of the billets will determine the heating temperature and the degree of deformation during welding, and, therefore, will affect the kinetics of austenite transformation in the thermomechanical influence area of welded joints and the mechanical properties of the joints that determine the reliability of drill pipes.

An analysis of literary sources has shown the existence of great interest in assessing the influence of the RFW parameters on the mechanical properties of joints of both homogeneous and dissimilar metals [6; 11; 12]. However, despite the abundance of published works, the information on rotary friction welding of carbon alloyed steels is limited. There are individual publications containing the results of studies of the microstructure and properties of welded joints of drill pipes made of N80 steels after normalisation with 42CrMo4 steel after quenching and tempering [13], AISI 8630 steel [9], welded joints of ASTM A 106 Grade B steel in the hot-rolled condition and AISI 4140 steel after normalisation and after quenching and tempering [5; 10]. These works indicate that the mechanical properties of welded joints during tensile tests with correctly selected welding conditions are not inferior to, and in some cases even surpass, the mechanical properties of the least durable of the mating materials. However, except for the tensile properties, an important issue for drill pipes is the assessment of brittle fracture resistance, namely the impact toughness of welded joints. Little attention is paid to the study of this parameter in the presented publications. For example, in the work [5], it is noted that the weld seam has lower impact toughness values compared to the original ASTM A 106 Grade B and AISI 4140 steels. However, no studies of the influence of the RFW parameters on the impact toughness value are presented in the analysed publication. In the work [9], the impact toughness values of AISI 8630 steel joints obtained with different parameters of inertia friction welding are presented. However, no comparison with microstructural changes in the weld zone is given.

It is known that the visco-plastic properties of steels largely depend on the morphological features of the phase microstructure components [14–16], which, as shown above, are determined by the welding parameters.

The aim of this work is to evaluate the influence of the structural-phase state formed in the joint area of steels under different friction forces during rotary friction welding on the impact toughness and the mechanism of destruction of welded joints of 32HGMA and 40HN2MA steels used for the production of drill pipes.

METHODS

The ingoing materials in this work were 32HGMA steel of S strength group according to API 5DP and 40HN2MA steel in the form of hot-rolled seamless pipes with an outside diameter of 73 mm and a wall thickness of 9 mm. The chemical composition of the selected steels, obtained using a Labspark 1000 optical emission spectrometer, is given in Table 1.

For 32HGMA steel, preliminary heat treatment included quenching from 870 °C and tempering at 580 °C with water cooling in a sprayer. For 40HN2MA steel, heat treatment consisted of normalisation at 880 °C, quenching from 860 °C with cooling in a water-polymer mixture, tempering at 580 °C with air cooling. The mechanical properties of the materials after heat treatment are given in Table 2.

Friction welding was performed using a 60-ton machine manufactured by Thompson Friction Welding company. The welding modes are given in Table 3. In this work, the friction force was varied while the forging force, rotation speed, and axial shortening were kept constant.

Some of the friction-welded samples were tempered at 550 °C for an hour in an SNOL chamber furnace.

The microstructure was studied on transverse sections after etching with a 4 % solution of nitric acid in ethanol. The macrostructure was studied using an Olympus DSX1000 optical microscope (Japan). The microstructure

Table 1. *Chemical composition of steels, wt. %*
Таблица 1. *Химический состав сталей, мас. %*

Steel grade	C	Mn	Si	S	P	Cr	Ni	Cu	Mo
32HGMA	0.32	0.82	0.36	0.005	0.010	0.98	0.15	0.14	0.31
40HN2MA	0.44	0.49	0.25	0.005	0.008	0.72	1.24	0.20	0.14

Table 2. *Mechanical properties of 32HGMA and 40HN2MA steels after heat treatment*
Таблица 2. *Механические свойства сталей 32ХГМА и 40ХН2МА после термической обработки*

Steel	Yield strength, MPa	Ultimate strength, MPa	Relative elongation, %	KCV, J/cm^2
32HGMA	777–792	894–907	14.5–15.5	87.5–92.4
40HN2MA	870–885	984–998	10.5–11.0	73.8–78.9

Table 3. *Rotary friction welding parameters*
Таблица 3. *Параметры ротационной сварки трением*

Mode (sample) No.	Force during friction, kN	Rotation frequency during friction, rpm	Force during forging, kN	Upset during welding, mm
1	100	600	220	7
2	145			

and fractographic analysis of the samples after impact bending tests were studied using a Tescan Mira 3 scanning electron microscope (Japan) at an accelerating voltage of 5 kV. The analysis of the steel interface using the electron backscatter diffraction (EBSD) method was carried out on a ThermoScience Scios 2 LoVac scanning electron microscope (Japan) with an Oxford Instrument Symmetry EBSD Detector attachment (Japan) using the AZtec software package. The microscope parameters at the time of shooting were as follows: accelerating voltage is 20 kV, probe current is 410 nA, and scanning step is 0.1 μm.

To determine the proportion of residual austenite in samples near the welded joint, X-ray structural analysis was used. The studies were carried out on a DRON-3M diffractometer (Russia) using copper K_α radiation at an accelerating voltage of 40 kV, a current force of 30 A, in the angular range of 30...90° with automatic data recording. The volume fraction of austenite was calculated from the ratio of the integral intensities of the diffraction lines J(III) of austenite and J(II0) of ferrite using the formula:

$$A_{res},\% = \frac{100}{\frac{J(\text{II}0)\alpha}{J(\text{III})\gamma} \times 0.742 + 1},$$

where A_{res} is the fraction of residual austenite;
J(II0)α is the intensity of the ferrite diffraction line;
J(III)γ is the intensity of the austenite diffraction line.

Charpy impact bending tests on samples with a V-type stress concentrator were carried out on a WANCE PIT-100 pendulum impact tester (China). The samples for determining impact toughness had dimensions of 5×10×55 mm. The stress concentrator was applied in the zone of junction of two steels. Impact toughness values were determined as the average value of three identical samples.

RESULTS

Microstructure

Fig. 1 shows photographs of the macrostructure of welded joints produced with different friction forces. Approximately the same volume of upset metal (burr) on the side of both steels indicates their similar mechanical properties at elevated temperatures. In both samples, three characteristic zones are distinguished in the welding area: the joint zone, the thermomechanically affected zone (TMAZ), and the heat-affected zone (HAZ). This is followed by the base metal zone. The thermomechanical effect zone is characterised by structural heterogeneity caused by the influence of the thermo-deformation cycle

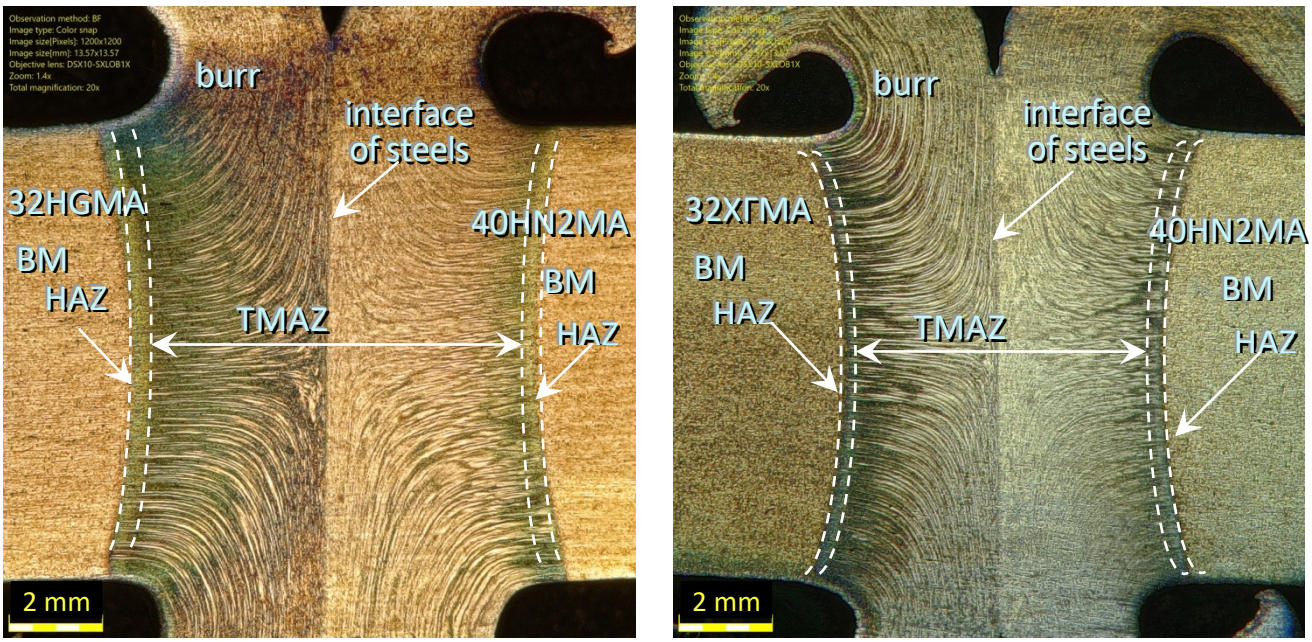

a *b*

Fig. 1. *Macrostructure of welded joint of 32HGMA and 40HN2MA steels produced by rotary friction welding:* ***a*** *– sample No. 1;* ***b*** *– sample No. 2.*
BM – base metal; TMAZ – thermomechanically affected zone; HAZ – heat-affected zone
Рис. 1. *Макроструктура сварного соединения сталей 32ХГМА и 40ХН2МА, полученного ротационной сваркой трением:* ***а*** *– образец № 1;* ***b*** *– образец № 2.*
ВМ – основной металл; TMAZ – зона термомеханического влияния; HAZ – зона термического влияния

of welding, as well as by plastic deformation of the metal during welding and the texture of the metal of the original pipes produced by hot rolling. Near the joint, an area with a parallel arrangement of fibres relative to the plane of contact of the billets can be distinguished. It is followed by a partially deformed zone where the texture threads are curved. This zone is followed by a zone with texture lines parallel to the rolling plane of the pipe billet. Such a structure of the welded joint was also observed in [10]. With increasing friction force, the total TMAZ length decreased from 7.7 mm in sample No. 1 to 6.7 mm in sample No. 2.

Fig. 2 and 3 show photographs of the microstructure of the welded joint interface. It is evident that there is no clear boundary between the steels, which in turn indicates the formation of common austenite grains during joint recrystallisation during welding. The resulting microstructure is predominantly acicular, indicating that the austenite transformation occurred in the low-temperature region. The size of the former austenite grain reaches 40 μm. At the same time, the inner structure of the austenite grains is highly fragmented; it consists of individual sections of crystallites elongated in one direction. The presence of a developed substructure is caused by the processes of dynamic recrystallisation of austenite during welding.

The kinetics of the deformed austenite transformation in the studied samples differs due to differences in the morphology of the phase components of the formed microstructure. In the microstructure of sample No. 1 obtained with a lower friction force, the microstructure of upper bainite and martensite was formed within one austenite grain (Fig. 2 d). Martensite areas are characterised by an acicular structure and strong misorientation of crystallites. Obviously, the γ→α transformation in them occurred at the final stage in carbon-rich areas.

The nucleation and growth of martensite crystals occurred both from the boundaries and from the subboundaries of deformed austenite. The formation of upper bainite is observed mainly on the side of 32HGMA steel. Morphologically, two types of upper bainite can be identified in the microstructure, differing in the structural features of the carbide phase. In one case, it has an elongated plate-like shape and is continuously located at the boundaries of ferrite laths. In the other case, the carbide phase is concentrated inside the grains of bainitic ferrite with a particle size of 0.1–0.2 μm. Obviously, in the first case, bainite has a coarser structure and is formed at higher transformation temperatures.

In sample No. 2 obtained with a higher friction force, only two morphological components of the α-phase are present in the microstructure of the interface: lamellar bainite and lath martensite. Elongated crystals of lath bainite, 5–15 μm in size, grouped into packets, formed in the lower temperature range of the γ→α transformation are morphologically close to martensite. The microstructure on the side of both steels is identical.

The study using EBSD analysis allowed identifying that the formation of a bainitic microstructure at low values of friction force led to a decrease in the proportion of high-angle boundaries (Fig. 2 c). A developed substructure of a reticular structure formed by low-angle boundaries is

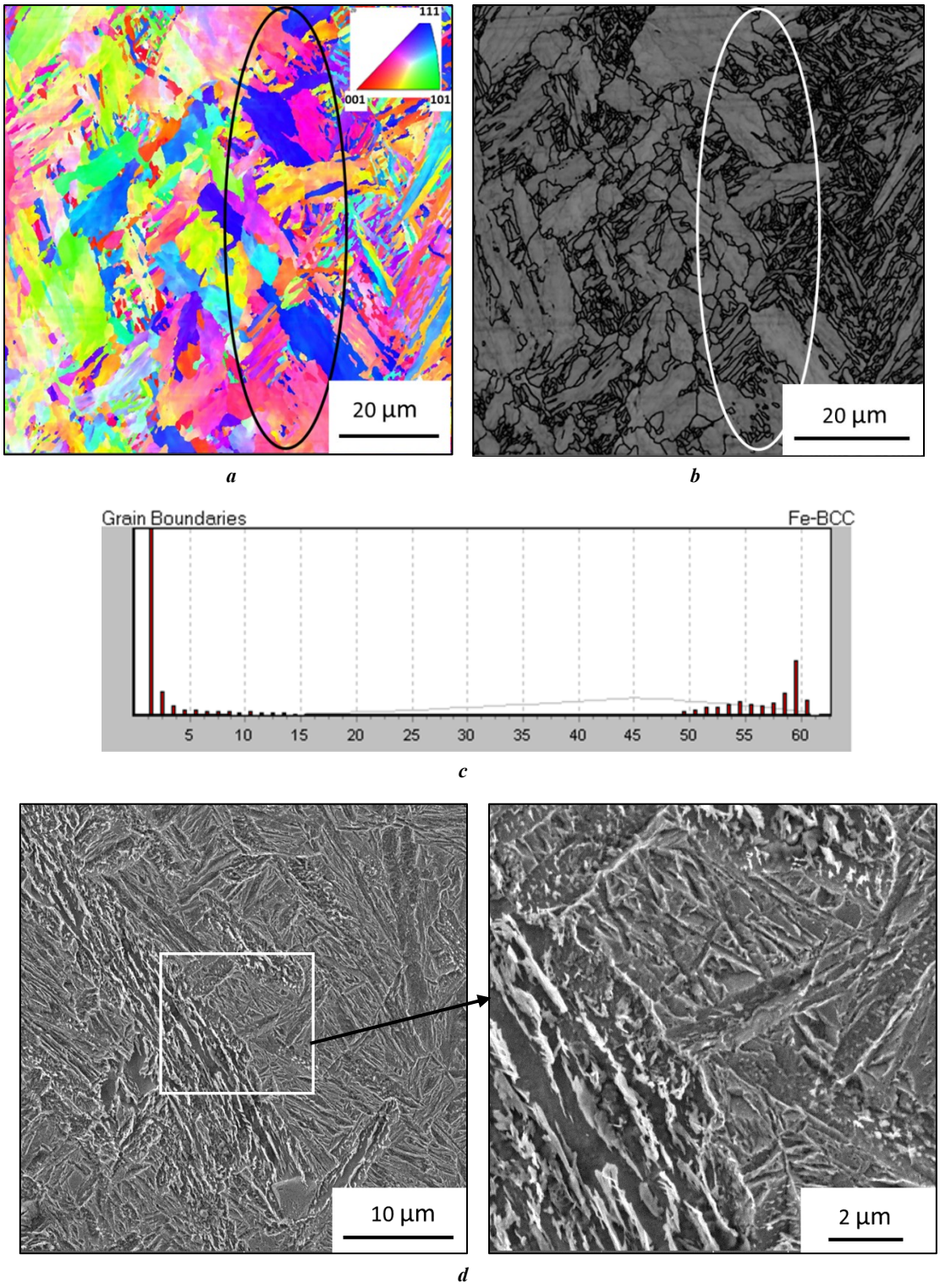

Fig. 2. *Microstructure of the interface of 32HGMA and 40HN2MA steels in a welded joint produced by rotary friction welding, mode No. 1:*
a *– crystallographic misorientation map;* ***b*** *– microstructure with high-angle boundaries (15°);*
c *– spectra of intercrystalline boundaries;* ***d*** *– SEM image*
Рис. 2. *Микроструктура зоны сопряжения сталей 32ХГМА и 40ХН2МА в сварном соединении, полученном ротационной сваркой трением, режим № 1:*
a *– карта кристаллографических разориентировок;* ***b*** *– микроструктура с нанесением большеугловых границ (15°);*
c *– спектры межкристаллитных границ;* ***d*** *– СЭМ-изображение*

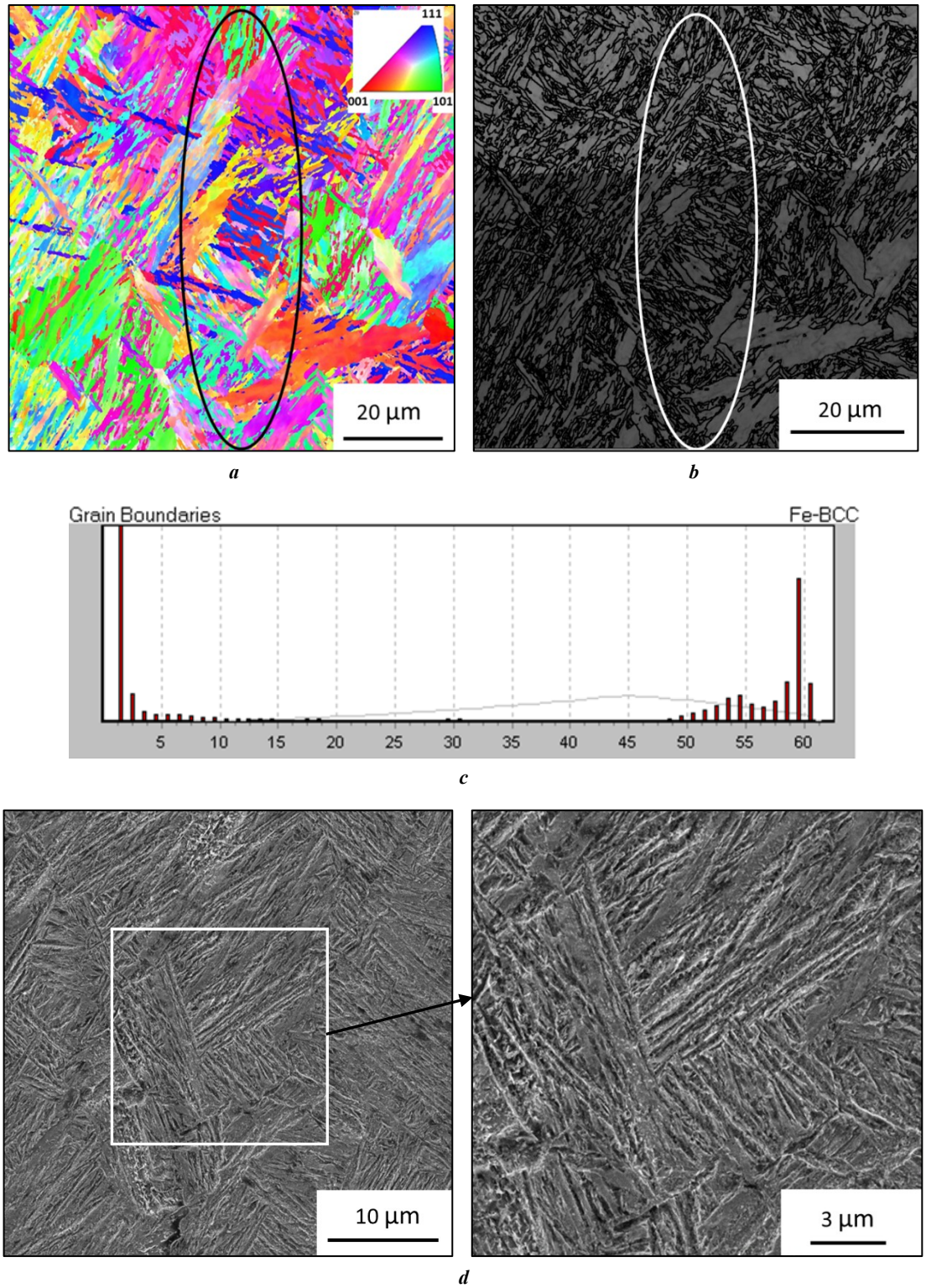

Fig. 3. *Microstructure of the interface of 32HGMA and 40HN2MA steels in a welded joint produced by rotary friction welding, mode No. 2:*
a *– crystallographic misorientation map;* ***b*** *– microstructure with high-angle boundaries (15°);*
c *– spectra of intercrystalline boundaries;* ***d*** *– SEM image*
Рис. 3. *Микроструктура зоны сопряжения сталей 32ХГМА и 40ХН2МА в сварном соединении, полученном ротационной сваркой трением, режим № 2:*
a *– карта кристаллографических разориентировок;* ***b*** *– микроструктура с нанесением большеугловых границ (15°);*
c *– спектры межкристаллитных границ;* ***d*** *– СЭМ-изображение*

observed inside the bainitic ferrite grains. At the same time, the lath morphology of the α-phase microstructure formed at higher friction force values is characterised by a higher density of high-angle boundaries located at misorientation angles from 49 to 60° (Fig. 3 c).

The proportion of residual austenite in the steel interface was determined by X-ray structural analysis. It was found that residual austenite in the amount of 2–3 % was detected in sample No. 2 welded at a higher friction force. In sample No. 1, the proportion of residual austenite is less than 1 %.

Post-welding tempering resulted in the development of diffusion processes with additional formation of carbide phases both inside and along the boundaries of the initial α-phase (Fig. 4, 5). In the structure of the upper bainite of tempered sample No. 1, a breakdown and partial coagulation of long cementite plates is observed (Fig. 4). In the martensitic microstructure areas, finely dispersed carbide particles precipitated. Thus, the structure of this sample after tempering is characterised by a combination of areas of a coarse bainitic structure with large carbides and areas of a more homogeneous dispersed structure.

In the microstructure of the mating zone of tempered sample No. 2, areas of a coarse structure are absent (Fig. 5). In the bainitic structure, a developed subgrain structure is observed in the α-phase crystals. The microstructure is homogeneous. Carbide particles are located both along the boundaries of the initial α-phase and inside the crystallites.

Microhardness

Fig. 6 shows the microhardness profiles in welded joints in the initial state and after tempering.

In the TMAZ, the microhardness changes abruptly, which is caused by the heterogeneity of the microstructure due to the presence of isolated areas of austenite decomposition products of different morphology. The highest microhardness values are observed in the TMAZ on the side of 40HN2MA steel in the as-welded state. In this case, the maximum value of 677 HV was recorded in the sample produced with a higher friction force. A tendency towards a decrease in microhardness is observed with distance from the mating zone. In the HAZ, the microhardness values are virtually identical to the values of the original steels, which were 271–288 HV for 32HGMA steel and 310–347 HV for 40HN2MA steel. The influence of tempering results in a decrease in microhardness in the TMAZ to values in the range of 256–424 HV, which is associated with a decrease in the tetragonality of the martensite crystal lattice and the precipitation of carbide particles.

Impact toughness

The results of determining the impact toughness in the steel interface zone are shown in Table 4, and the fractograms of the tested samples are shown in Fig. 7.

In the as-welded state, the steel interface zone has a low toughness reserve, which is determined by the brittleness of the microstructures formed in this zone. In all cases, fracture occurred along the body of the former austenite grain. However, some differences are observed in the morphology of the fracture surface of the samples produced with different friction forces. The fracture surface of the sample produced using mode No. 1 has virtually no traces of plastic deformation. The fracture mechanism is cleaving (Fig. 7 a). The facets of the transcrystalline cleavage are relatively flat areas disordered relative to the adjacent facets by a certain angle. Secondary cracks extending deep into the sample are revealed perpendicular to the direction of growth of the main crack.

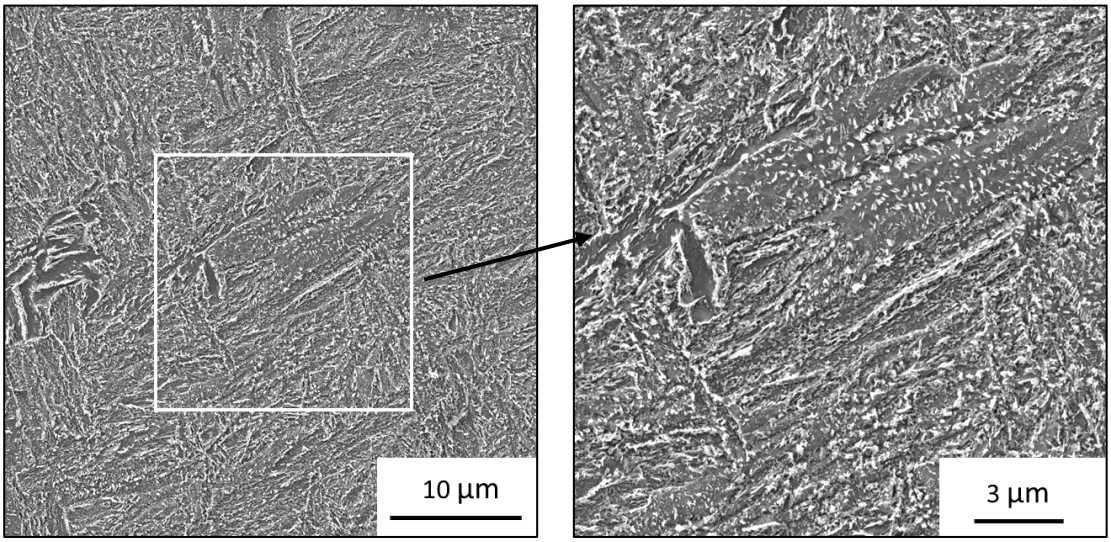

Fig. 4. *Microstructure of the interface of the welded joint of 32HGMA and 40HN2MA steels after tempering at 550 °C for 1 h, welding mode No. 1*
Рис. 4. *Микроструктура зоны сопряжения сварного соединения сталей 32ХГМА и 40ХН2МА после отпуска при 550 °С в течение 1 ч, режим сварки № 1*

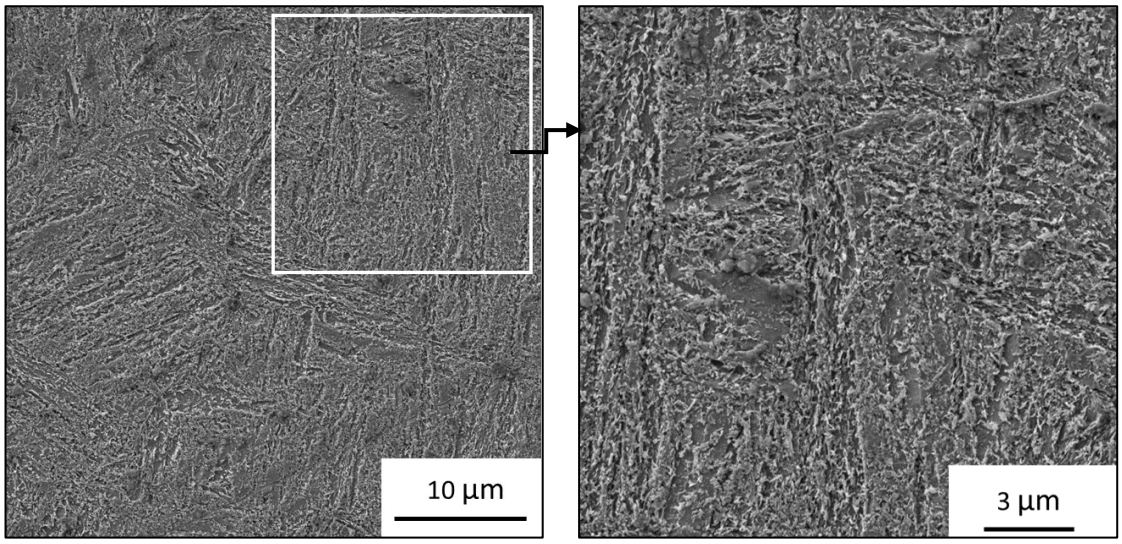

Fig. 5. *Microstructure of the interface of the welded joint of 32HGMA and 40HN2MA steels after tempering at 550 °C for 1 h, welding mode No. 2*
Рис. 5. *Микроструктура зоны сопряжения сварного соединения сталей 32ХГМА и 40ХН2МА после отпуска при 550 °С в течение 1 ч, режим сварки № 2*

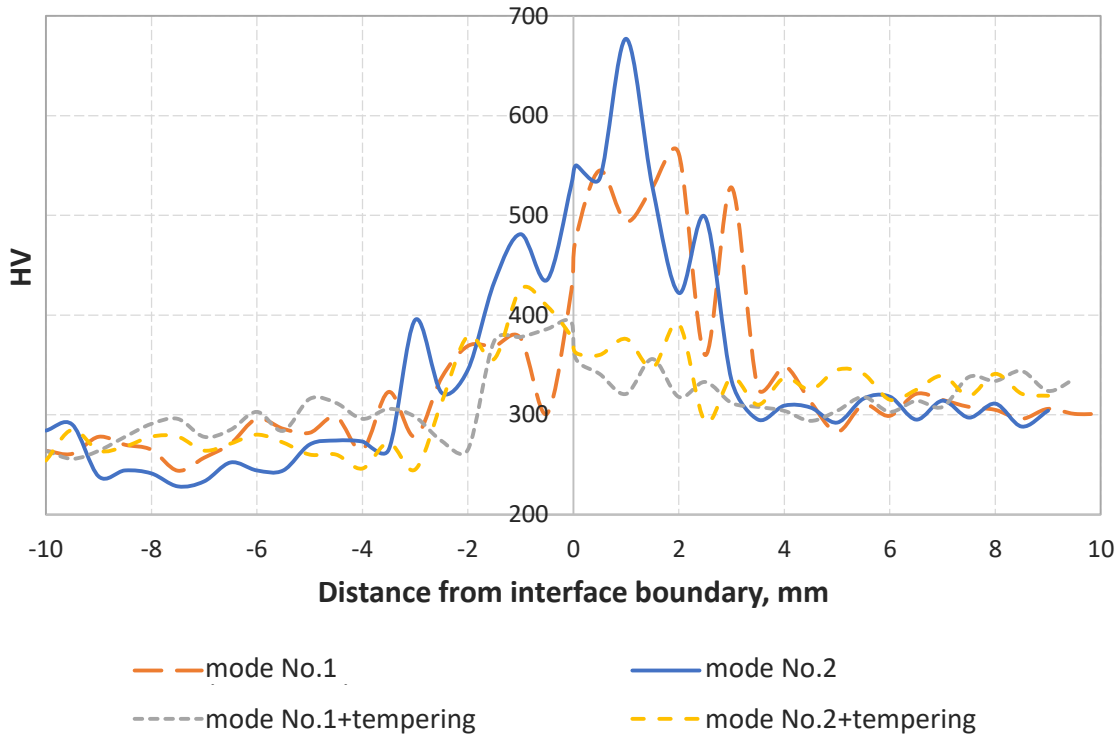

Fig. 6. *Microhardness profiles in welded joints in the initial state and after tempering*
Рис. 6. *Профили микротвердости в сварных соединениях в исходном состоянии и после отпуска*

The sample produced using mode No. 2 fractured with a greater share of plastic deformation. The fracture macrostructure is characterised by the formation of a small contraction at the edges. In the microrelief, the quasi-cleavage micromechanism dominates. The quasi-cleavage facets alternate with the dimple structure (Fig. 7 c).

Tempering contributed to an increase in the impact toughness of the welded joints. In this case, the maximum value of KCV=53.5 J/cm^2 is recorded in sample No. 2 produced with a higher friction force. Traces of macroplastic deformation in the form of the formation of shear lips are observed on the fracture surface of this sample (Fig. 7 d).

Table 4. *Impact toughness of the interface in welded joints of 32HGMA and 40HN2MA steels*
Таблица 4. *Ударная вязкость зоны сопряжения в сварных соединениях сталей 32ХГМА и 40ХН2МА*

Welding mode	No. 1	No. 2	No. 1 + tempering	No. 2 + tempering
KCV, J/cm^2	11.3	18.0	19.3	53.5

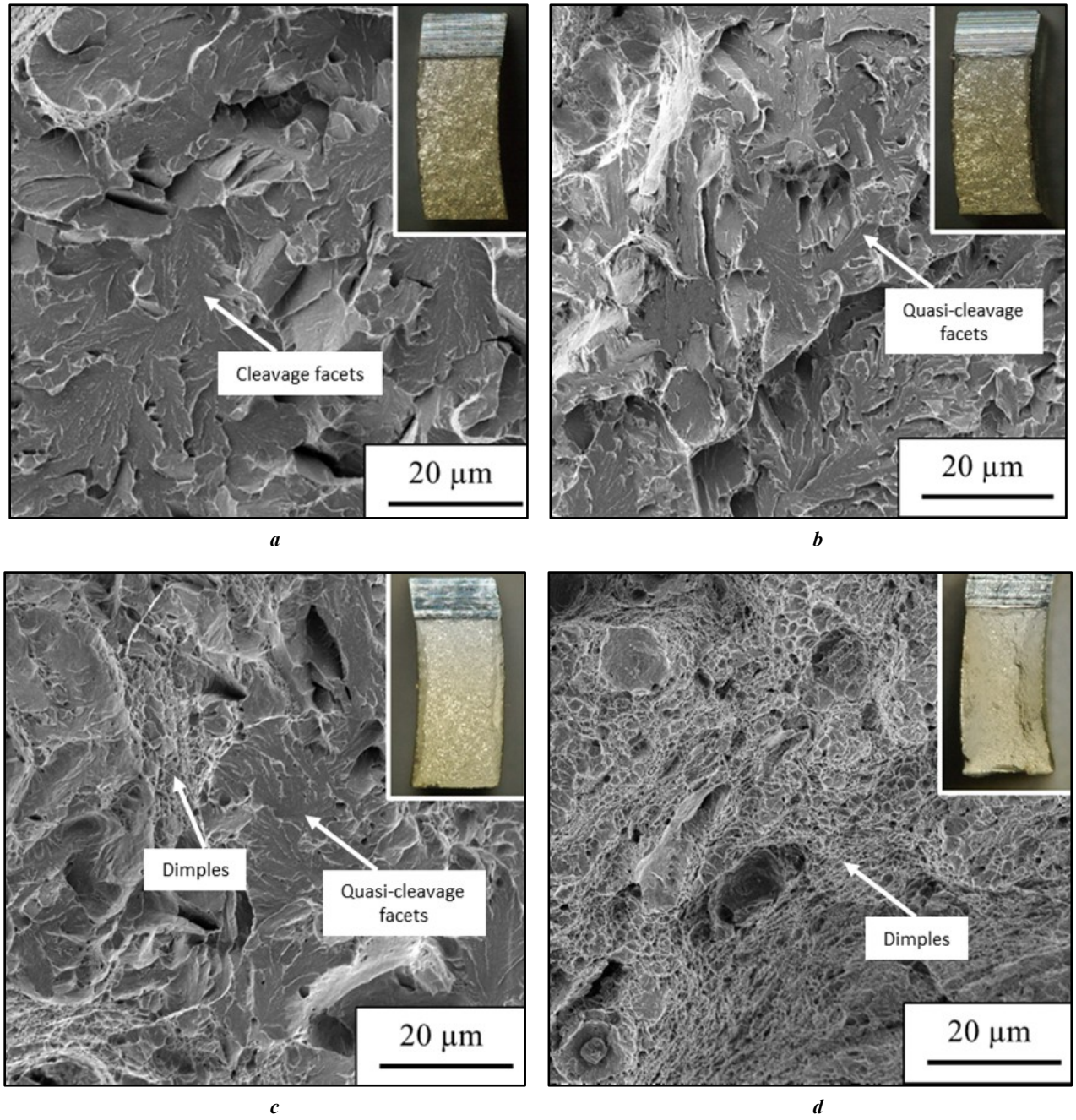

Fig. 7. *Fractograms of samples of welded joint of 32HGMA and 40HN2MA steels after impact bending tests:*
a *– mode No. 1;* ***b*** *– mode No. 1 + tempering;* ***c*** *– mode No. 2;* ***d*** *– mode No. 2 + tempering*
Рис. 7. *Фрактограммы образцов сварных соединений сталей 32ХГМА и 40ХН2МА после испытаний на ударный изгиб:*
a *– режим № 1;* ***b*** *– режим № 1 + отпуск;* ***c*** *– режим № 2;* ***d*** *– режим № 2 + отпуск*

The fracture morphology is completely represented by dimples of ductile fracture. Against the background of a fine-dimple microrelief, individual large dimples are observed, the centres of origin of which are large particles.

In the tempered sample of the welded joint produced with a lower friction force, the impact toughness increased insignificantly compared to the initial state. The crack propagated in this case according to the quasi-cleavage mechanism (Fig. 7 b). The fracture surface has a more developed surface structure compared to the state of this sample after welding and more pronounced ridges of separation in the locations of high-angle boundaries. No secondary cracks were detected.

DISCUSSION

The results of the conducted studies confirmed the assumption about the influence of the RFW parameter (force at the friction stage) on the microstructure and toughness of the mating zone of medium-carbon alloyed steels. This is related to the fact that with an increase in the friction force, the temperature and degree of deformation of the near-contact zones of the billets increase, which is consistent with the results of modelling the RFW process presented in works [17–19]. These conditions, apparently, led to the suppression of the formation of coarse-acicular bainite in the upper temperature range of the transformation. The formation of a coarse microstructure of upper bainite with a large number of large cementite particles, obtained at a lower force during friction of the billets, causes brittleness of the microstructure, which is not eliminated by subsequent high-temperature tempering. The negative effect of upper bainite on impact toughness was previously noted in studies [20–22]. The authors of the work [5] note as well the relationship between low impact toughness in the joint interface and the presence of coarse carbide particles at the interface, which does not contradict the results obtained in this work.

Thus, an increase in the force of friction of the billets at the stage of their heating in the RFW process leads to an increase in the visco-plastic properties of the interface of steels after high-temperature tempering of welded joints. This effect is achieved due to the formation of a more homogeneous fine-grained microstructure of tempered martensite and lower bainite with a developed subgrain structure.

CONCLUSIONS

1. In welded joints of 32HGMA and 40HN2MA medium-carbon alloyed steels produced by rotary friction welding, a microstructure consisting of sections of martensite and bainite of various morphologies is formed in the steel interface. The morphology of the bainitic component of the microstructure depends on the welding parameters and the kinetics of the transformation of supercooled austenite.

2. It was found that at reduced values of the force during friction of the billets after the completion of welding, in the steel interface, a coarse microstructure of upper bainite with uneven precipitation of large carbide particles is formed, which negatively affects the visco-plastic properties of the steel interface.

3. With an increase in the force at the stage of friction of the billets after the completion of welding, the formation of a more dispersed structure of lath bainite and an increase in the density of high-angle boundaries occur. After high tempering, such a microstructure provides high impact toughness in the interface of steels due to the transformation into a tempered bainite structure with a developed subgrain structure.

4. The toughness of the interface of steels can be controlled by welding modes, avoiding the need for complete subsequent recrystallisation of the weld zone (quenching and tempering), which significantly reduces the cost of manufacturing of high-strength drill pipes.

REFERENCES

1. Ovchinnikov D.V., Sofrygina O.A., Zhukova S.Y., Pyshmintsev I.Y., Bityukov S.M. Influence of microalloying with boron on the structure and properties of high-strength oil pipe. *Steel in Translation*, 2011, vol. 41, no. 4, pp. 356–360. DOI: 10.3103/S0967091211040188.
2. Sofrygina O.A., Zhukova S.Y., Bityukov S.M., Pyshmintsev I.Y. Economical steels for the manufacture of high-strength oil pipe (according to the API Spec5CT standard). *Steel in Translation*, 2010, vol. 40, no. 7, pp. 616–621. DOI: 10.3103/S0967091210070041.
3. Zaselskiy E.M., Tikhontseva N.T., Savchenko I.P., Sofrygina O.A. Development and implementation of materials in the production of high-strength drill pipes with special properties. *Problemy chernoy metallurgii i materialovedeniya*, 2021, no. 2, pp. 37–40. EDN: XBMMOL.
4. Still J.R. Welding of AISI 4130 and 4140 steels for drilling systems. *Welding Journal*, 1997, vol. 76, no. 6, pp. 37–42.
5. Khadeer Sk.A., Babu P.R., Kumar B.R., Kumar A.S. Evaluation of friction welded dissimilar pipe joints between AISI 4140 and ASTM A 106 Grade B steels used in deep exploration drilling. *Journal of Manufacturing Processes*, 2020, vol. 56, part A, pp. 197–205. DOI: 10.1016/j.jmapro.2020.04.078.
6. Maalekian M. Friction Welding-Critical Assessment of Literature. *Science and Technology of Welding and Joining*, 2007, no. 12, pp. 738–759. DOI: 10.1179/174329307X249333.
7. Vill V.I. *Svarka metallov treniem* [Friction welding of metals]. Moscow, Mashinostroenie Publ., 1970. 176 p.
8. Li Wenya, Vairis A., Preuss M., Ma Tiejun. Linear and Rotary Friction Welding Review. *International Materials Reviews*, 2016, no. 61, pp. 71–100. DOI: 10.1080/09506608.2015.1109214.
9. Banerjee A., Ntovas M., Da Silva L., Rahimi S., Wynne B. Inter relationship between microstructure evolution and mechanical properties in inertia friction welded 8630 low-alloy steel. *Archives of Civil and Mechanical Engineering*, 2021, vol. 21, article number 149. DOI: 10.1007/s43452-021-00300-9.

10. Kumar A.S., Khadeer Sk.A., Rajinikanth V., Pahari S., Kumar B.R. Evaluation of bond interface characteristics of rotary friction welded carbon steel to low alloy steel pipe joints. *Materials Science & Engineering A*, 2021, vol. 824, article number 141844. DOI: 10.1016/j.msea.2021.141844.
11. Shete N., Deokar S.U. A Review Paper on Rotary Friction Welding. *International Conference on Ideas, Impact and Innovation in Mechanical Engineering*, 2017, vol. 5, no. 6, pp. 1557–1560.
12. Cai Wayne, Daehn G., Vivek A., Li Jingjing, Khan H., Mishra R.S., Komarasamy M. A State of the Art Review on Solid-State Metal Joining. *Journal of Manufacturing Science and Engineering*, 2019, vol. 141, no. 3, article number 031012. DOI: 10.1115/1.4041182.
13. Emre H.E., Kaçar R. Effect of Post Weld Heat Treatment Process on Microstructure and Mechanical Properties of Friction Welded Dissimilar Drill Pipe. *Materials Research*, 2015, vol. 18, no. 3, pp. 503–508. DOI: 10.1590/1516-1439.308114.
14. Kaletin A.Y., Kaletina Y.V., Ryzhkov A.G. Enhancement of impact toughness of structural steels upon formation of carbide-free bainite. *Physics of Metals and Metallography*, 2015, vol. 116, no. 1, pp. 109–114. DOI: 10.1134/S0031918X15010068.
15. Maisuradze M.V., Kuklina A.A., Nazarova V.V., Ryzhkov M.A., Antakov E.V. Microstructure and mechanical property formation of heat treated low-carbon chromium-nickel-molybdenum steels. *Metallurgist*, 2024, vol. 68, no. 3, pp. 322–335. DOI: 10.1007/s11015-024-01732-3.
16. Panin V.E., Shulepov I.A., Derevyagina L.S., Panin S.V., Gordienko A.I., Vlasov I.V. Nanoscale mesoscopic structural states in low-alloy steels for martensitic phase formation and low-temperature toughness enhancement. *Physical mesomechanics*, 2020, vol. 23, no. 5, pp. 376–383. DOI: 10.1134/S1029959920050021.
17. Celik S., Ersozlu I. Investigation of the mechanical properties and microstructure of friction welded joints between AISI 4140 and AISI 1050 steels. *Materials and Design*, 2009, vol. 30, no. 4, pp. 970–976. DOI: 10.1016/j.matdes.2008.06.070.
18. Nan Xujing, Xiong Jiangtao, Jin Feng, Li Xun, Liao Zhongxiang, Zhang Fusheng, Li Jinglong. Modeling of rotary friction welding process based on maximum entropy production principle. *Journal of Manufacturing Processes*, 2019, vol. 37, pp. 21–27. DOI: 10.1016/j.jmapro.2018.11.016.
19. Geng Peihao, Qin Guoliang, Zhou Jun. Numerical and experimental investigation on friction welding of austenite stainless steel and middle carbon steel. *Journal of Manufacturing Processes*, 2019, vol. 47, pp. 83–97. DOI: 10.1016/j.jmapro.2019.09.016.
20. Kaletin A.Yu., Schastlivtsev V.M., Kareva N.T., Smirnov M.A. Embrittlement of structural steel with bainitic structure during tempering. *Fizika metallov i metallovedenie*, 1983, vol. 56, no. 2, pp. 366–371. EDN: TBDJOQ.
21. Zikeev V.N., Chevskaya O.N., Mishet'yan A.R., Filippov V.G., Korostelev A.B. Effect of high strength structural steel structural state on fracture resistance. *Metallurgist*, 2021, vol. 65, no. 3-4, pp. 375–388. DOI: 10.1007/s11015-021-01167-0.
22. Kaletin A.Yu., Kaletina Yu.V., Simonov Yu.N. Retained austenite and impact strength of structural steels with carbide-free bainite. *Bulletin of PNRPU. Mechanical engineering, materials science,* 2022, vol. 24, no. 4, pp. 49–55. EDN: UZSBWG.

СПИСОК ЛИТЕРАТУРЫ

1. Ovchinnikov D.V., Sofrygina O.A., Zhukova S.Y., Pyshmintsev I.Y., Bityukov S.M. Influence of microalloying with boron on the structure and properties of high-strength oil pipe // Steel in Translation. 2011. Vol. 41. № 4. P. 356–360. DOI: 10.3103/S0967091211040188.
2. Sofrygina O.A., Zhukova S.Y., Bityukov S.M., Pyshmintsev I.Y. Economical steels for the manufacture of high-strength oil pipe (according to the API Spec5CT standard) // Steel in Translation. 2010. Vol. 40. № 7. P. 616–621. DOI: 10.3103/S0967091210070041.
3. Засельский Е.М., Тихонцева Н.Т., Савченко И.П., Софрыгина О.А. Разработка и освоение материалов в производстве высокопрочных бурильных труб со специальными свойствами // Проблемы черной металлургии и материаловедения. 2021. № 2. С. 37–40. EDN: XBMMOL.
4. Still J.R. Welding of AISI 4130 and 4140 steels for drilling systems // Welding Journal. 1997. Vol. 76. № 6. P. 37–42.
5. Khadeer Sk.A., Babu P.R., Kumar B.R., Kumar A.S. Evaluation of friction welded dissimilar pipe joints between AISI 4140 and ASTM A 106 Grade B steels used in deep exploration drilling // Journal of Manufacturing Processes. 2020. Vol. 56. Part A. P. 197–205. DOI: 10.1016/j.jmapro.2020.04.078.
6. Maalekian M. Friction Welding-Critical Assessment of Literature // Science and Technology of Welding and Joining. 2007. № 12. P. 738–759. DOI: 10.1179/174329307X249333.
7. Вилль В.И. Сварка металлов трением. М.: Машиностроение, 1970. 176 с.
8. Li Wenya, Vairis A., Preuss M., Ma Tiejun. Linear and Rotary Friction Welding Review // International Materials Reviews. 2016. № 61. P. 71–100. DOI: 10.1080/09506608.2015.1109214.
9. Banerjee A., Ntovas M., Da Silva L., Rahimi S., Wynne B. Inter relationship between microstructure evolution and mechanical properties in inertia friction welded 8630 low-alloy steel // Archives of Civil and Mechanical Engineering. 2021. Vol. 21. Article number 149. DOI: 10.1007/s43452-021-00300-9.
10. Kumar A.S., Khadeer Sk.A., Rajinikanth V., Pahari S., Kumar B.R. Evaluation of bond interface characteristics of rotary friction welded carbon steel to low alloy steel pipe joints // Materials Science & Engineering A. 2021. Vol. 824. Article number 141844. DOI: 10.1016/j.msea.2021.141844.
11. Shete N., Deokar S.U. A Review Paper on Rotary Friction Welding // International Conference on Ideas, Im-

pact and Innovation in Mechanical Engineering. 2017. Vol. 5. № 6. P. 1557–1560.
12. Cai Wayne, Daehn G., Vivek A., Li Jingjing, Khan H., Mishra R.S., Komarasamy M. A State of the Art Review on Solid-State Metal Joining // Journal of Manufacturing Science and Engineering. 2019. Vol. 141. № 3. Article number 031012. DOI: 10.1115/1.4041182.
13. Emre H.E., Kaçar R. Effect of Post Weld Heat Treatment Process on Microstructure and Mechanical Properties of Friction Welded Dissimilar Drill Pipe // Materials Research. 2015. Vol. 18. № 3. P. 503–508. DOI: 10.1590/1516-1439.308114.
14. Калетин А.Ю., Рыжков А.Г., Калетина Ю.В. Повышение ударной вязкости конструкционных сталей при образовании бескарбидного бейнита // Физика металлов и металловедение. 2015. Т. 116. № 1. С. 114–120. DOI: 10.7868/S0015323015010064.
15. Майсурадзе М.В., Куклина А.А., Назарова В.В., Рыжков М.А., Антаков Е.В. Формирование микроструктуры и механических свойств при термической обработке низкоуглеродистых хромоникельмолибденовых сталей // Металлург. 2024. № 3. С. 21–30. DOI: 10.52351/00260827_2024_3_21.
16. Панин В.Е., Шулепов И.А., Деревягина Л.С., Панин С.В., Гордиенко А.И., Власов И.В. Создание наномасштабных мезоскопических структурных состояний для образования мартенситных фаз в низколегированной стали с целью получения высокой низкотемпературной ударной вязкости // Физическая мезомеханика. 2019. Т. 22. № 6. С. 5–13. EDN: ZGEIOJ.
17. Celik S., Ersozlu I. Investigation of the mechanical properties and microstructure of friction welded joints between AISI 4140 and AISI 1050 steels // Materials and Design. 2009. Vol. 30. № 4. P. 970–976. DOI: 10.1016/j.matdes.2008.06.070.
18. Nan Xujing, Xiong Jiangtao, Jin Feng, Li Xun, Liao Zhongxiang, Zhang Fusheng, Li Jinglong. Modeling of rotary friction welding process based on maximum entropy production principle // Journal of Manufacturing Processes. 2019. Vol. 37. P. 21–27. DOI: 10.1016/j.jmapro.2018.11.016.
19. Geng Peihao, Qin Guoliang, Zhou Jun. Numerical and experimental investigation on friction welding of austenite stainless steel and middle carbon steel // Journal of Manufacturing Processes. 2019. Vol. 47. P. 83–97. DOI: 10.1016/j.jmapro.2019.09.016.
20. Калетин А.Ю., Счастливцев В.М., Карева Н.Т., Смирнов М.А. Охрупчивание конструкционной стали с бейнитной структурой при отпуске // Физика металлов и металловедение. 1983. Т. 56. № 2. С. 366–371. EDN: TBDJOQ.
21. Зикеев В.Н., Чевская О.Н., Мишетьян А.Р., Филиппов В.Г., Коростелев А.Б. Влияние структурного состояния конструкционных высокопрочных сталей на сопротивление разрушению // Металлург. 2021. № 4. С. 15–25. DOI: 10.52351/00260827_2021_04_15.
22. Калетин А.Ю., Калетина Ю.В., Симонов Ю.Н. Остаточный аустенит и ударная вязкость конструкционных сталей с бескарбидным бейнитом // Вестник Пермского национального исследовательского политехнического университета. Машиностроение, материаловедение. 2022. Т. 24. № 4. С. 49–55. EDN: UZSBWG.

Взаимосвязь микроструктуры и ударной вязкости зоны сопряжения сварных соединений сталей 32ХГМА и 40ХН2МА, полученных ротационной сваркой трением

Приймак Елена Юрьевна*[1,2,4], кандидат технических наук, доцент,
заведующий лабораторией металловедения и термической обработки,
директор научно-образовательного центра новых материалов и перспективных технологий
Атамашкин Артём Сергеевич[2,5], кандидат технических наук,
старший научный сотрудник научно-образовательного центра новых материалов и перспективных технологий
Яковлева Ирина Леонидовна[3,6], доктор технических наук,
главный научный сотрудник лаборатории физического металловедения
Фот Андрей Петрович[1,7], доктор технических наук, профессор,
главный ученый секретарь – начальник отдела диссертационных советов
[1]*АО «Завод бурового оборудования», Оренбург (Россия)*
[2]*Оренбургский государственный университет, Оренбург (Россия)*
[3]*Институт физики металлов имени М.Н. Михеева Уральского отделения РАН, Екатеринбург (Россия)*

***E-mail:** e.prijmak@zbo.ru

[4]ORCID: https://orcid.org/0000-0002-4571-2410
[5]ORCID: https://orcid.org/0000-0003-3727-8738
[6]ORCID: https://orcid.org/0000-0001-8918-3066
[7]ORCID: https://orcid.org/0000-0002-2971-7908

Поступила в редакцию 27.02.2025 *Пересмотрена 21.03.2025* *Принята к публикации 10.04.2025*

Аннотация: Настоящая работа посвящена оценке влияния морфологических особенностей микроструктуры среднеуглеродистых легированных сталей, сформированной при различном усилии в процессе ротационной сварки трением (РСТ), на ударную вязкость их зоны сопряжения. Приведены результаты экспериментального исследования соединения, полученного при сварке трубных заготовок из сталей 32ХГМА и 40ХН2МА с внешним диаметром 73 мм и толщиной стенки 9 мм при изменении силы на этапе трения (разогрева) заготовок. Исследования микроструктуры, микротвердости и ударной вязкости на образцах с *V*-образным надрезом сварных соединений были проведены в исходном состоянии после сварки и после отпуска при температуре 550 °С. Проведен макро- и микрофрактографический анализ разрушенных образцов. Показано, что сила при трении оказывает влияние на кинетику фазовых превращений, фазовый состав и однородность микроструктуры в зоне сопряжения сталей. С уменьшением данного параметра РСТ возрастает неоднородность микроструктуры, связанная с возникновением участков верхнего бейнита с неравномерными выделениями крупных карбидных частиц, что оказывает негативное влияние на вязкость зоны сопряжения сталей как в исходном состоянии, так и после отпуска; механизм разрушения – квазискол. При более высоких значениях силы при трении повышается плотность большеугловых границ и дисперсность микроструктуры бейнита, что обеспечивает более высокую вязкость и энергоемкость разрушения с формированием ямочного микрорельефа. Полученные результаты открывают возможности регулирования вязкопластических свойств сварных соединений уже на этапе сварки без последующей перекристаллизации зоны сварного шва.

Ключевые слова: ротационная сварка трением; среднеуглеродистые легированные стали; зона сопряжения сварных соединений; мартенсит; бейнит; ударная вязкость.

Благодарности: Исследование выполнено за счет гранта Российского научного фонда № 23-79-01311, https://rscf.ru/project/23-79-01311.

Электронно-микроскопические исследования с применением метода дифракции обратно рассеянных электронов выполнены в ИФМ УрО РАН в Центре коллективного пользования «Испытательный центр нанотехнологий перспективных материалов».

Исследования с использованием сканирующего электронного микроскопа Tescan Mira 3 проводились в Центре коллективного пользования Центра выявления и поддержки одаренных детей «Гагарин» (Оренбургская область).

Для цитирования: Приймак Е.Ю., Атамашкин А.С., Яковлева И.Л., Фот А.П. Взаимосвязь микроструктуры и ударной вязкости зоны сопряжения сварных соединений сталей 32ХГМА и 40ХН2МА, полученных ротационной сваркой трением // Frontier Materials & Technologies. 2025. № 2. С. 73–85. DOI: 10.18323/2782-4039-2025-2-72-6.